Differentiation of rat dermal mesenchymal cells and calcification in three-dimensional cultures

Taiki Suyama[1], Mitsutoki Hatta[2], Shozaburo Hata[1], Hiroyuki Ishikawa[1], Jun Yamazaki[2 *]

Departments of [1)]Oral Growth & Development, and [2)]Physiological Science & Molecular Biology, Fukuoka Dental College, Sawara-ku, Fukuoka 814-0193, Japan

*Corresponding author: Jun Yamazaki, Ph.D.
Department of Physiological Science & Molecular Biology, Fukuoka Dental College
2-15-1 Tamura, Sawara-ku, Fukuoka 814-0193, Japan
Tel.: 81-92-801-0411 ext. 669; Fax: 81-92-801-4909
E-mail: junyama@college.fdcnet.ac.jp

Running title: Ectopic calcification of rat dermal 3-D cultures

Abstract

Three-dimensional (3-D) cultures are known to promote cell differentiation. Previously, we investigated the differentiation of rat dermal fibroblasts to α-smooth muscle actin (α-SMA)-positive myofibroblasts through transforming growth factor (TGF)-β production using a 3-D culture model. Here, we investigated the phenotypic change from dermal mesenchymal cells (mostly fibroblasts) to osteoblast-like cells, being inspired by the roles of smooth muscle cells or fibroblasts during vascular calcification. Spindle-shaped cells that grew in heterologous populations out of dermal explants from 2-day-old Wistar rats were cultured within a collagen matrix. α-SMA and alkaline phosphatase (ALP) mRNA levels initially increased, followed by a rise in Runx2 and osteocalcin (OCN) mRNA levels without calcification. Calcium deposits were produced in the presence of a high concentration of inorganic phosphate (2.1 mM) or β-glycerophosphate (βGP, 10 mM) after 2 weeks of culture, and both were sensitive to an inhibitor of type III phosphate transporters. An ALP inhibitor decreased only βGP-induced calcification. Inhibition of TGF-β type-I receptors attenuated ALP mRNA levels and βGP-induced calcification, suggesting that endogenous TGF-β stimulates ALP activity and then βGP breakdown. An increase in the number of cells embedded in the collagen gel enhanced the mRNA levels of Runx2 and OCN, but not of ALP. Collectively, several factors are likely to promote the differentiation of dermal mesenchymal cells into osteoblast-like cells and ectopic calcification in a 3-D collagen matrix, implying the utility of these cells as a potential autologous cell source for

tissue engineering.

Key words: three-dimensional culture, dermis, alkaline phosphatase, TGF-β, calcification

1. Introduction

The function of most mammalian cells is dependent on their interaction with neighboring cells and the extracellular matrix (ECM) [1]. Three-dimensional (3-D) cultures are reportedly capable of offering technical advantages in that osteoblasts are sensitive to various factors that modify their proliferation and differentiation [2]. Previously, we investigated the mechanism underlying the regulation of myofibroblastic differentiation using a 3-D reconstruction model derived from neonatal rat skin [3]. Myofibroblasts are characterized by their *de novo* expression of α-smooth muscle actin (α-SMA), which generates a contractile force in granulation tissue [4], and transforming growth factor (TGF)-βs are known to act as stimulators of such differentiation [5]. Our previous study revealed that the endogenous secretion of TGF-β1 was involved in the effective expression of α-SMA in dermal myofibroblasts in an autocrine or paracrine fashion [3].

Intriguingly, in the 2-D environment, relatively undifferentiated fibroblasts can exhibit a particular phenotype (osteogenic, chondrogenic, or adipogenic) in response to microenvironmental factors to which they are exposed [6,7]. Conversely, myofibroblasts are capable of differentiating into other types of cells including osteoblasts and adipocytes following the addition of bone morphogenetic or differentiation-inducing substances [8,9]. In rat dermal fibroblasts, TGF-β1 promotes osteogenic as well as myofibroblastic differentiation, i.e., an increase in the expression levels of alkaline phosphatase (ALP) and osteocalcin (OCN) as early and late osteoblast differentiation markers, respectively [10]. In analogy with the

promotion of the osteogenic potential of osteoblast-like cells in the presence of 3-D cell-to-cell contact [11], a heterogeneous population of dermal fibroblasts/myofibroblasts is expected to be amenable to culture in a 3-D environment and to gain the potential to undergo osteoblastic differentiation.

Inorganic phosphate (Pi) has emerged as an indispensable regulator of calcification. Similar to the *in vivo* vascular calcification caused by hyperphosphatemia, elevated Pi (2 mM) has been shown to stimulate ALP and OCN expression, and to calcify the ECM in human aortic smooth muscle cell culture [12]. The addition of Pi stimulates the autocrine loop of TGF-β1 production that induces the expression of OCN and Runx2, a key transcriptional regulator of bone matrix proteins, in vascular smooth muscle cells [13]. Thus, we hypothesized that dermal mesenchymal cells (mostly fibroblasts) in 3-D cultures also undergo phenotypic changes effectively with the aid of the endogenous production of TGF-β1, and cause calcification in the presence of elevated Pi or the phosphate donor β-glycerophosphate (βGP).

The aim of this study was to investigate the potential of phenotypic transformation to osteoblast-like cells of mesenchymal cells including fibroblasts outgrown from rat dermal explants using 3-D culture and to clarify the mechanism underlying such an osteogenic response. This basic approach may lay the groundwork for future tissue engineering applications for osteogenic regeneration.

2. Materials and Methods

2.1 Antibodies and reagents

The antibodies used were primarily mouse monoclonal anti-α-SMA (clone 1A4; Dako, Glostrup, Denmark), rabbit polyclonal anti-TGF-β1 (G122A; Promega, Madison, WI), mouse monoclonal anti-OCN (6-7H; TaKaRa Bio., Shiga, Japan), rabbit polyclonal anti-dentin matrix protein-1 (DMP-1) (M176; TaKaRa), rabbit polyclonal anti-CD44 (bs-0521R; Bioss, Inc., Woburn, MA), and rabbit polyclonal anti-CD90/Thy-1 (bs-0778R; Bioss). LY364947 (Cayman Chemical, Ann Arbor, MI) was dissolved in dimethyl sulfoxide to make a stock solution, which was further diluted more than 1,000 fold before use. Levamisole HCl was obtained from Santa Cruz Biotech. (CA, USA). All other compounds were from Sigma-Aldrich Co. (St. Louis, MO).

2.2 Dissociation of rat dermal mesenchymal cells and construction of the collagen gel matrix culture

Two-day-old Wistar rats were killed with anesthetic isoflurane. The dorsal skin was disinfected with ethanol and removed. The experimental procedures were approved by the Animal Research Committee of Fukuoka Dental College. The skin was incubated overnight at 4°C in modified Eagle's medium containing dispase (750 protease units/mL, Dispase II; Godo Shusei, Tokyo, Japan). Dermal tissue was minced into rectangular pieces and cultured in Dulbecco's modified Eagle's medium (DMEM) containing 15% fetal bovine serum (FBS). Cells that sprouted from the dissected dermis were

collected by digesting spindle-shaped cells surrounding the tissue explant at 37°C for 5 min in phosphate-buffered saline containing 0.1% trypsin and 0.65 mM EDTA. FBS was added to stop enzyme activity. The cells were centrifuged, resuspended in fresh medium containing 10% FBS, and cultured for 5–6 days. They were then subcultured twice.

Collagen gels were prepared according to previously published methods [3]. Briefly, type-I collagen (0.725 volume; Nitta Gelatin, Osaka, Japan) was mixed on ice with a reconstitution buffer (0.1 volume; 2.2 g $NaHCO_3$ and 4.77 g HEPES in 100 mL of 50 mmol/L NaOH, pH 7.0), 5-times concentrated DMEM (without $NaHCO_3$, 0.15 volume), and 10-times concentrated Ham's F-12 medium (without $NaHCO_3$, 0.025 volume). A total of 2.5 mL of gel was mixed with 1.25×10^5 (1×) or 5.0×10^5 (4×) cells and poured into a cell culture insert (3.0-cm diameter, Millicell CM; Millipore, Temecula, CA). The gel was warmed at 37°C for 30 min to solidify it and produce 3-D cultures. The culture insert was placed in an outer dish (10-cm diameter) containing DMEM supplemented with 10% FBS, and then incubated at 37°C in 5% CO_2. After one week, the culture medium was changed to α-MEM supplemented with 10% FBS. New culture medium was added every three days. Unless otherwise indicated, the concentration of Pi in the culture medium was 1.0 mM. The 3-D culture was maintained in α-MEM for 2 weeks. The concentration of Pi in the presence of βGP was measured using a molybdenum blue visual colorimetric method (WAK-PO_4(C); Kyoritsu Chemical-Check Lab., Tokyo, Japan).

2.3 ALP and Alizarin Red staining

Cells embedded in collagen gel were fixed with a fixative solution (45% acetone- and 10% methanol-containing citrate buffer; pH 5.4) for 5 min and then washed several times with distilled water. The cells were then stained by incubation with nitro blue tetrazolium chloride and bromo-chloro-indolyl phosphate at 37°C for 10 min to detect ALP activity (TRACP & ALP double-stain kit; Takara Bio.). For the detection of calcification, cultures were stained with 0.5% Alizarin Red S solution (Sigma-Aldrich Co.) for 1.5 min. Quantification of the relative intensity of the staining (in arbitrary units) was performed with the aid of ImageJ software (NIH, Bethesda, MD).

2.4 Real-time PCR measurement of mRNA levels

mRNA was measured using PCR as described previously [3]. Briefly, Total RNA was isolated from dermal cells (mostly fibroblasts/myofibroblasts) in the 3-D-reconstruction model, and mRNA was reverse transcribed into cDNA. Samples were analyzed in duplicate by quantitative PCR with the comparative $\Delta\Delta C_T$ method (Applied Biosystems 7500 Real-time PCR System; Grand Island, NY) with SYBR^R Premix Ex Taq II (Takara Bio.) Specific primers to target genes and an endogenous control, β-actin (ACTB) (Table 1) were used under the following thermal cycling conditions: 95°C, 5 s; 60°C, 30 s; and 72°C, 45 s for 40 cycles. Mean ΔC_T in the control group was used as an internal calibrator, and the relative quantity of the target gene in the test groups was calculated as $2^{-\Delta\Delta C_T}$ (range = $2^{-(\Delta\Delta C_T - S)}$ to $2^{-(\Delta\Delta C_T + S)}$), where S is the standard error of the mean (SEM) of the $\Delta\Delta C_T$ value.

2.5 Immunofluorescence

The 3-D culture was fixed with 4% paraformaldehyde overnight at 4°C and then permeabilized with 0.1% Triton X-100 for 5 min at room temperature. The culture was incubated with 10% goat serum for 1 h, followed by a 2-h incubation with an anti-α-SMA (1:200), -TGF-β1 (1:200), -OCN (1:100), -DMP-1 (1:100), -CD44 (1:100), or -CD90 (1:100) antibody, and a 1-h incubation with an anti-rabbit or anti-mouse IgG antibody (1:800) conjugated with Alexa Fluor 488 or 594 (Molecular Probes, Inc., Eugene, OR). Fluorescence was observed using a fluorescence microscope (BZ-9000; Keyence, Osaka, Japan).

2.6 Statistical analysis

All values are presented as the mean ± SEM (N, number of observations). Statistical analysis for the comparison of 2 groups was performed using a paired *t*-test. For more than 3 groups, analysis was performed using one-way analysis of variance for a randomized block experiment followed by a *post hoc* Fisher's PLSD test. A P-value less than 0.05 was considered statistically significant.

3. Results

3.1 Three-dimensional culture of dermis-derived cells causes a time-dependent increase in the expression of osteogenic genes

A large number of spindle-shaped cells sprouted from the tissue sections

dissected from rat dermis. With increasing time in 2-D culture, the fibroblasts changed to exhibit a flattened shape (Fig. 1A). Some of these cells had positive immunoreactivity to α-SMA, a myofibroblast marker after the outgrowth. Furthermore, positive staining for ALP activity was observed in some cells even in the 2-D culture. Many cells appeared to be positive for the dermal multipotent cell markers CD44 and CD90/Thy-1 [14,15] (Fig. 1B); however, it is reportedly difficult to distinguish dermal multipotent cells from fibroblasts [6,7].

After being subcultured twice in flasks containing DMEM, the cells were dissociated and embedded in a collagen gel matrix. The 3-D culture medium was DMEM for 1 week and then changed to α-MEM containing a normal concentration of Pi (1.0 mM) (Fig. 1C). The α-SMA and ALP mRNA levels during the initial incubation in DMEM were already almost 50–60% of those detected at 2 weeks after changing the medium to α-MEM. These levels increased during the early period of incubation in α-MEM to reach the maximum level detected for 1 to 2 weeks (Fig. 2A). Staining for ALP activity exhibited a similar time course with the mRNA levels (Fig. 2B, 2C).

However, the time course of Runx2 and OCN mRNA levels was entirely distinct from that of ALP mRNA. They were less than 30% during the initial incubation in DMEM, and increased gradually during the period of incubation in α-MEM (Fig. 2A). Being consistent with our previous study [3], immunostaining revealed the initial diffuse production of TGF-β1 protein in the 3-D culture and the existence of relatively large α-SMA-positive cells with a polygonal shape, although α-SMA-negative cells were also found (Fig.

2D). While TGF-β1 production decreased in the later period, α-SMA-positive cells still remained in the culture. Neither the late osteoblast marker OCN nor the osteocyte marker DMP-1 was expressed during incubation in DMEM. However, the number of small polygonal cells gradually increased, expressing both OCN and DMP-1 and extending processes to neighboring cells after the medium was switched to α-MEM. Most cells did not express both α-SMA and DMP-1 (Fig. 2D).

3.2 Pi and βGP stimulate calcification in 3-D culture of rat dermis-derived cells

When we investigated the existence of calcium deposits in epi-illumination images of the 3-D cultures, they were barely detected in the presence of the normal concentration of Pi (1.0 mM). Remarkably, at 2 weeks after the addition of a high concentration of Pi (1.1 mM; final concentration, 2.1 mM) and βGP (10 mM), the epi-illumination images of representative gels demonstrated reflective white deposits in the 3-D culture. High Pi and βGP concentrations substantially increased Alizarin Red staining (Fig. 3). Without the cells embedded, high Pi never produced deposits or increased Alizarin Red staining. High Pi and βGP slightly increased the mRNA expression of ALP, but not of Runx2 or OCN (Fig. 4). These results suggest that both inorganic and organic phosphates stimulated calcification in some biological process without altering the transcription of Runx2 and OCN.

To clarify the mechanisms underlying the calcification induced by adding high Pi and βGP concentrations, the roles of phosphate transporters

and alkaline phosphatase were investigated. An inhibitor of type III phosphate transporters, phosphonoformic acid (PF, 1 mM) [16], abolished both high Pi- and βGP-induced Alizarin Red staining (Fig. 5A) without altering ALP mRNA levels (Fig. 6). In contrast, the ALP inhibitor levamisole (Lev, 1 mM), which is known to have no effect on phosphate transport [17], inhibited βGP-induced calcification, whereas it failed to alter the Pi-induced action (Fig. 5B). Lev did not induce significant changes in ALP mRNA levels (Fig. 6). To confirm the breakdown of βGP into Pi, we measured the increase of Pi concentration in culture medium supplemented with 10 mM βGP for 3 days culture of the dermis-derived cells. The increased Pi concentration was estimated to be 1.13 ± 0.09 mM (n = 4). These results indicate that the action of both high Pi and βGP concentrations requires PF-sensitive phosphate transporters, while the latter also requires ALP activity to degrade the compound into Pi.

3.3 Expression of ALP and the subsequent βGP-induced calcification is dependent on endogenous TGF-β

Previously, we reported that rat dermal fibroblasts in a 3-D culture secreted TGF-β1 (in both active and latent forms) to change their phenotype to the contractile form (myofibroblasts), suggesting the involvement of the basal release of TGF-β1 in the cell differentiation process [3]. In that study, a TGF-β type-I receptor inhibitor, LY364947 (3 μM) [18], attenuated α-SMA production in myofibroblasts. At 2 weeks after continual 3-D culture in α-MEM, LY364947 at the same concentration significantly attenuated the

mRNA expression of ALP, but not that of Runx2 or OCN (Fig. 7A). Conversely, recombinant TGF-β1 (4 ng/mL) did not modify the expression of ALP, Runx2, or OCN mRNA (data not shown). These observations suggest that endogenous TGF-β appeared to be sufficient to stimulate ALP expression and to be irrelevant for the transcription of Runx2 and OCN in the present study.

According to the results shown above, it is assumed that endogenous TGF-β promotes βGP-induced calcification through an increase in ALP activity. While inhibiting ALP mRNA levels (Fig. 7A) even in the presence of high Pi or βGP, LY364947 (3 μM) significantly suppressed the βGP-induced Alizarin Red staining, whereas it failed to alter the Pi-induced staining, suggesting a role for endogenous TGF-β in calcification induced only by βGP through the upregulation of ALP activity (Fig. 7B).

3.4 Expression of Runx2 or osteocalcin, but not that of alkaline phosphatase, is dependent on cell density in 3-D culture

The aforementioned results indicate that Runx2 and OCN expression is unlikely to be regulated by TGF-β, in contrast to ALP expression and βGP-induced calcification. Thus, we considered that other signaling pathways should promote the expression of Runx2 and related genes. Interestingly, when the number of cells embedded in the collagen gel was increased by 4 fold, Runx2 and OCN mRNA levels were significantly increased, whereas ALP mRNA levels and βGP-induced calcification were unaltered (Fig. 8), suggesting cell density-dependent signaling is involved in the enhanced transcription of Runx2 and related genes.

4. Discussion

The present study demonstrated that in 3-D culture of cells outgrown from rat dermis, mRNA and protein levels related to the osteogenic response increase with differential time courses and that calcium deposits are produced in the presence of inorganic or organic phosphates with the aid of phosphate transporters and ALP. This phenotypic change is likely to be promoted by endogenous TGF-β levels and cell density.

The existence of fibroblast heterogeneity has been well documented [19]. Dermal fibroblasts contain heterogeneous cell populations including stem cells with various levels of differentiation potential and fibroblasts with no capacity to convert to other cell types [7]. Thus, the spindle cells that sprouted from the rat dermal tissue explants should consist of heterogeneous populations, and a subpopulation of dermis-derived multipotent cells could be involved in the differentiation capacity to generate the osteoblastic phenotype. The profiles of the specific surface antigen phenotype such as CD44 and CD90 are similar in mesenchymal stem cells and dermal fibroblasts [6,7]. Therefore, further study through clonal analysis has to be conducted to determine which specific biomarkers the outgrown cells express and which cells have the potential to undergo phenotypic change in the present 3-D culture.

Type I collagen, the main organic component of bone matrix, enhances osteoblastic differentiation and bone formation [11]. Notably, rat primary osteoblasts growing in 3-D cultures of collagen gels increased the expression

of osteoblastic genes [2]. In analogy, we embedded cells that sprouted from rat dermal explants in a 3-D culture of collagen gel, and expected the specific cell differentiation. In fact, ALP mRNA expression was almost half of the maximal level within 1 week and reached the maximal level for 1 to 2 weeks, while both Runx2 and OCN mRNA gradually increased within 2 weeks. These differential time courses indicate that these genes are expressed in different populations of dermal fibroblasts and/or regulated separately in the same population of cells. The former idea is more likely to be supported by the present immunocytochemistry study showing the expression of α-SMA with OCN and DMP-1 in different cells embedded in the 3-D culture.

Previously, we reported that the basal release of endogenous TGF-β1 effectively promotes α-SMA production in the 3-D culture of fibroblasts/myofibroblasts in autocrine and paracrine manners [3]. TGF-β1 is widely considered to be a key regulator of the differentiation of many different cell types and to play an important role in bone metabolism because it affects both osteoblast and osteoclast cell lineages [20]. In the present study, the endogenous production of TGF-β1 is likely to be involved, at least, in the expression of ALP, since LY364947 inhibited ALP mRNA levels; however, it barely affected Runx2 and OCN mRNA levels. Conflicting data have been shown concerning the effects of TGF-β1 on gene expression in osteoblast progenitors. TGF-β1 has been shown to increase the expression of Runx2, osteopontin, OCN, and collagen type I [13]. Conversely, TGF-β1 promotes the early stage of differentiation, whereas it blocks the later stages of differentiation and mineralization [20]. In the present 3-D culture, since

the endogenous production of TGF-β1 was detected in the early period, the TGF-β1-induced action on ALP expression is likely to be highlighted.

A high Pi environment is reportedly needed for the ectopic calcification of vascular smooth muscle cell culture [13]. Several types of Pi transporters are involved in the phosphate carriers important for ECM calcification [21]. The type III NaPi transporters Pit-1/Glvr-1 and Pit-2/Ram-1 are expressed by most cell types [22]. Mineralization was upregulated with the overexpression of Pit-1 in osteoblast culture [23]. Jono et al. [12] reported that the type III NaPi transporter expressed in human vascular smooth muscle cells was identified as Pit-1 and that the specific inhibitor PF inhibited the Pi-induced deposition of calcium. Further evaluation using RNA interference confirmed the involvement of Pit-1 in vascular smooth muscle cell calcification [24]. In the present study, we found that the NaPi transporter inhibitor attenuated the Pi- and βGP-produced deposition of calcium in myofibroblast cultures, suggesting an indispensable role of NaPi transporters. In contrast, the tissue-nonspecific ALP inhibitor Lev reduced βGP-induced calcification, but not Pi-induced calcification, through the inhibition of ALP activity. These results are consistent with a previous report for human osteoblast-like SaOS-2 cells [25], except for the limited action of Lev on transcription. βGP serves as a phosphate source for bone minerals [26]. ALP plays a key role in mineralization by degrading βGP into Pi [25]. In fact, we confirmed the increase in Pi in the βGP-containing culture medium for the myofibroblast-derived cells, being consistent with a previous report using culture of mouse MC3T3-E1 osteoblast-like cells (4.8 mM Pi after 48 h

culture) [27]. Furthermore, LY364947 inhibited βGP-induced calcification, but not high Pi-induced calcification. These results suggest that Pi is presumably supplied during the calcification process by the breakdown of βGP by ALP that has been upregulated by TGF-β in 3-D culture.

Previous studies have reported the entry of Pi into cells affects the expression of osteogenic genes. Pi activated the ERK signaling pathway and had an effect on osteogenic gene expression [28]. Pi increased Runx2 and OCN mRNA levels in vascular smooth muscle cells [12,29]. Pi and βGP increased ALP mRNA and ALP activity in SaOS-2 osteoblast-like cells [25]. In the present study, a slight but significant increase in ALP was detected in the presence of Pi and βGP, although no change was not observed for Runx2 and OCN expression as far as we tested using the dermis-derived cells. Although the expression of Runx2 and OCN was insensitive to the compounds that affected ALP mRNA levels, we found that their expression was dependent on cell density in the 3-D culture. Previously, it was reported that the seeded population of osteosarcoma cells in 3-D collagen scaffolds affected the degree of osteoblastic differentiation [30]. Cell-to-cell interactions, such as physical contact shown as cell processes extending to neighboring cells or the secretion of intercellular signaling molecules, should be considered when trying to understand the promotion of the osteogenic response in 3-D cultures.

In conclusion, endogenous TGF-β levels and cell density are likely to promote the differentiation of dermal mesenchymal cells, mostly fibroblasts, into osteoblast-like cells in a 3-D collagen matrix. In the presence of

inorganic or organic phosphate, the functions of phosphate transporters and phosphatases are likely to be necessary for the formation of calcium deposits. The present 3-D model is likely to offer an advantageous autologous cell source of tissue engineering for osteogenic regeneration. Further analysis should be performed to characterize the differentiation potential of the subpopulations of dermal mesenchymal cells to commit to an osteogenic lineage.

Acknowledgements

The authors are grateful to Drs. K. Kato, K. Okamura, and T. Ohkubo for their helpful discussions. We also thank Drs. K. Uehara and M. Segawa (Fukuoka University School of Medicine) for their support in the microscopy study. This study was supported by Grant-in-Aids for Challenging Exploratory Research (Grant Number 26670104) (J.Y.) and for Scientific Research (C) (Grant Number 25462906) (M.H) from the Japan Society for the Promotion of Science, and a Grant-in-Aid from the Ministry of Education, Culture, Sports, Science, and Technology-Supported Program for the Strategic Research Foundation at Private Universities (S1001059) (J.Y.).

Conflict of Interest

The authors have no financial conflict of interest.

Ethical statement

All institutional and national guidelines for the care and use of laboratory

animals were followed and approved by the institutional committee (see Materials and Methods).

References

1. Buttery L, Bielby R, Howard D, Shakesheff K. Osteogenic differentiation of embryonic stem cells in 2D and 3D culture. 3D Cell Culture: Methods and Protocols. In: Haycock JW, editor. Methods Mol Biol. Vol. 695. Springer Science+Business Media; 2011. p.281-308.

2. Matthews BG, Naot D, Callon KE, Musson DS, Locklin R, Hulley PA, et al. Enhanced osteoblastogenesis in three-dimensional collagen gels. BoneKEy Rep 2014;3:560.

3. Hata S, Okamura K, Hatta M, Ishikawa H, Yamazaki J. Proteolytic and non-proteolytic activation of keratinocyte-derived latent TGF-β1 induces fibroblast differentiation in a wound-healing model using rat skin. J Pharmacol Sci 2014;124:230-43.

4. Gabbiani G, Ryan GB, Majne G. Presence of modified fibroblasts in granulation tissue and their possible role in wound contraction. Experientia 1971;27:549-550.

5. Tomasek JJ, Gabbiani G, Hinz B, Chaponnier C, Brown RA. Myofibroblasts and mechano-regulation of connective tissue remodelling. Nat Rev Mol Cell Biol 2002;3:349-363.

6. Lorenz K, Sicker M, Schmelzer E, Rupf T, Salvetter J, Schulz-Siegmund M, et al. Multilineage differentiation potential of human dermal skin-derived fibroblasts. Exp Dermatol 2008;17:925-932.

7. Alt E, Yan Y, Gehmert S, Song Y-H, Altman A, Gehmert S, et al. Fibroblasts share mesenchymal phenotypes with stem cells, but lack their differentiation and colony-forming potential. Biol Cell 2011;103:197-208.

8. Cheng SL, Shao JS, Charlton-Kachigian N, Loewy AP, Towler DA. MSX2 promotes osteogenesis and suppresses adipogenic differentiation of multipotent mesenchymal progenitors. J Biol Chem 2003;278:45969-45977.

9. Shao JS, Cai J, Towler DA. Molecular mechanisms of vascular calcification: lessons learned from the aorta. Arterioscler Thromb Vasc Biol 2006;26:1423-1430.

10. Simionescu A, Simionescu DT, Vyavahare NR. Osteogenic responses in fibroblasts activated by elastin degradation products and transforming growth factor-β1: role of myofibroblasts in vascular calcification. Am J Pathol 2007;171:116-123.

11. Casser-Bette M, Murray AB, Closs EI, Erfle V, Schmidt J. Bone formation by osteoblast-like cells in a three-dimensional cell culture. Calcif Tissue Int 1990;46:46-56.

12. Jono S, McKee MD, Murry CE, Shioi A, Nishizawa Y, Mori K, et al. Phosphate regulation of vascular smooth muscle cell calcification. Circ Res 2000;87:E10-17.

13. Wang N, Wang X, Xing C, Sun B, Yu X, Hu J, et al. Role of TGF-β1 in bone matrix production in vascular smooth muscle cells induced by a high-phosphate environment. Nephron Exp Nephrol 2010;115:e60-8.

14. Shi C, Cheng. Effects of acute wound environment on neonatal rat dermal multipotent cells. Cells Tissues Organs 2003;175:177-185.

15. Hasebe Y, Hasegawa S, Hashimoto N, Toyoda M, Matsumoto K, Umezawa A, et al. Analysis of cell characterization using cell surface markers in the dermis. J Dermatol Sci 2011;62:98-106.

16. Loghman-Adham M, Szczepanska-Konkel M, Yusufi AN, Van Scoy M, Dousa TP. Inhibition of Na^+-P_i cotransporter in small gut brush border by phosphonocarboxylic acids. Am J Physiol 1987;252(2 Pt 1):G244-G249.

17. Montessuit C, Caverzasio J, Bonjour JP. Characterization of a Pi transport system in cartilage matrix vesicles. Potential role in the calcification process. J Biol Chem 1991;266:17791-17797.

18. Peng SB, Yan L, Xia X, Watkins SA, Brooks HB, Beight D, et al. Kinetic characterization of novel pyrazole TGF-β receptor I kinase inhibitors and their blockade of the epithelial-mesenchymal transition.
Biochemistry 2005;44:2293-2304.

19. Driskell RR, Watt FM. Understanding fibroblast heterogeneity in the skin. Trends Cell Biol 2015;25:92-99.

20. Janssens K, ten Dijke P, Janssens S, Van Hul W. Transforming growth factor-β1 to the bone. Endocr Rev 2005;26:743-774.

21. Caverzasio J, Bonjour JP. Characteristics and regulation of Pi transport in osteogenic cells for bone metabolism. Kidney Int 1996;49:975-980.

22. Kavanaugh MP, Miller DG, Zhang W, Law W, Kozak SL, Kabat D, et al. Cell-surface receptors for gibbon ape leukemia virus and amphotropic murine retrovirus are inducible sodium-dependent phosphate symporters. Proc Natl Acad Sci U S A 1994;91:7071-7075.

23. Yoshiko Y, Candeliere GA, Maeda N, Aubin JE. Osteoblast autonomous Pi regulation via Pit1 plays a role in bone mineralization. Mol Cell Biol 2007;27:4465-4474.

24. Li X, Yang HY, Giachelli CM. Role of the sodium-dependent phosphate

cotransporter, Pit-1, in vascular smooth muscle cell calcification. Circ Res 2006;98:905-912.

25. Orimo H, Shimada T. The role of tissue-nonspecific alkaline phosphatase in the phosphate-induced activation of alkaline phosphatase and mineralization in SaOS-2 human osteoblast-like cells. Mol Cell Biochem 2008;315:51-60.

26. Langenbach F, Handschel J. Effects of dexamethasone, ascorbic acid and β-glycerophosphate on the osteogenic differentiation of stem cells in vitro. Stem Cell Res Ther 2013;4:117.

27. Nakano Y, Addison WN, Kaartinen MT. ATP-mediated mineralization of MC3T3-E1 osteoblast cultures. Bone 2007;41:549-561.

28. Franceschi RT, Ge C, Xiao G, Roca H, Jiang D. Transcriptional regulation of osteoblasts. Ann N Y Acad Sci 2007;1116:196-207.

29. Hosaka N, Mizobuchi M, Ogata H, Kumata C, Kondo F, Koiwa F, et al. Elastin degradation accelerates phosphate-induced mineralization of vascular smooth muscle cells. Calcif Tissue Int 2009;85:523-529.

30. Bitar M, Brown RA, Salih V, Kidane AG, Knowles JC, Nazhat SN. Effect of cell density on osteoblastic differentiation and matrix degradation of biomimetic dense collagen scaffolds. Biomacromolecules 2008;9:129-135.

Figure legends

Figure 1. Characteristics of cells outgrown from rat dermal explants (**A**, **B**) and a schematic diagram of the 3-D culture. **A**, Spindle-shaped cells sprouted

from tissue sections dissected from rat dermis and cultured on a plastic plate for the indicated time. The hatched line denotes the edge of the tissue explant. P# denotes passage number. **B**, Immunostaining for α-SMA, a myofibroblast marker, and for the dermal multipotent cell markers CD44 and CD90/Thy-1, and staining for ALP activity. Green (G), CD44 and CD90; red (R), α-SMA; blue, nucleus (DAPI). **C**, The culture insert (3.0 cm ϕ) was placed in an outer dish (10 cm ϕ) together with DMEM for 1 week (upper) followed by α-MEM for 2 weeks (lower). Photographs of the inner dish and the 3-D culture at 2 weeks after changing to α-MEM are also shown.

Figure 2. Time courses of the relative levels of α-SMA, ALP, Runx2, and OCN mRNA (**A**), staining for ALP activity (**B** and **C**), and immunostaining for TGFβ-1, α-SMA, OCN, and DMP-1 proteins (**B**) in rat dermis-derived cells embedded in 3-D culture. Culture medium contained 1.0 mM Pi. **A,** The mean ΔC_T value at 2 weeks after changing the medium from DMEM to α-MEM was used as an internal calibrator. Numbers of experiments are shown in parentheses. **D**, Green (G), TGF-β1 and DMP-1; red (R), α-SMA and OCN; blue, nucleus (DAPI); Ph, phase-contrast image.

Figure 3. Calcification occurs in 3-D cultures of rat dermis-derived cells in the presence of high concentrations of Pi (1.1 mM added, 2.1 mM final) and βGP (10 mM). Normal culture medium contained 1.0 mM Pi. **A**, Left: epi-illumination images of representative gels show reflective white deposits in the 3-D cultures for 2 weeks. **A**, Right: Alizarin Red S staining shows

nodular deposits indicating calcification in predominantly extracellular regions. Calcium deposits were not found in the collagen gel without cells in the high Pi-medium. **B**, Intensity of Alizarin Red S staining (arbitrary units; a.u.) in the presence or absence of Pi and βGP. ***P < 0.001, compared with the corresponding value for control (Ctrl). Numbers of experiments are shown in parentheses.

Figure 4. Effects of high concentrations of Pi (1.1 mM added, 2.1 mM final) and βGP (10 mM) on the expression of ALP, Runx2, and OCN mRNA measured in rat dermis-derived cells embedded in 3-D culture. Normal culture medium contained 1.0 mM Pi. *P < 0.05, **P < 0.01: compared with the corresponding value for control (Ctrl). Numbers of experiments are shown in parentheses.

Figure 5. Differential effects of phosphonoformic acid (PF, 1 mM) and levamisole (Lev, 1 mM) on Alizarin Red S staining enhanced by high Pi (1.1 mM added, 2.1 mM final) or βGP (10 mM) in 3-D cultures of rat dermis-derived cells. Normal culture medium contained 1.0 mM Pi. **A**, Representative gels. **B**, Intensity of staining (arbitrary units; a.u.). *P < 0.05, **P < 0.01, ***P < 0.001, compared with the corresponding value. Numbers of experiments are shown in parentheses.

Figure 6. Effects of phosphonoformic acid (PF, 1 mM) and levamisole (Lev, 1 mM) on the expression of ALP mRNA measured in rat dermis-derived cells

embedded in 3-D culture in the presence of high Pi (1.1 mM added, 2.1 mM final) or βGP (10 mM). The mean ΔC_T value in the normal culture medium (1.0 mM Pi) without PF and Lev was used as an internal calibrator. No significant difference was observed in comparison with the corresponding value for control (Ctrl). Numbers of experiments are shown in parentheses.

Figure 7. Modulation by TGF-β signaling of the expression of ALP, Runx2, and OCN mRNA and Alizarin Red S staining in 3-D cultures of rat dermis-derived cells. **A**, Effects of LY364947 (LY, 3 μM) in culture medium containing 1.0 mM Pi (upper) and in medium containing 2.1 mM Pi or 10 mM βGP (lower). **B**, Representative gels (upper) and intensity of staining (arbitrary units; a.u.) (lower). *P < 0.05, ***P < 0.001, compared with the corresponding value. Numbers of experiments are shown in parentheses.

Figure 8. Effects of cell density on the relative expression of ALP, Runx2, and OCN mRNA, and on Alizarin Red S staining in the presence of βGP (10 mM). The collagen gel was mixed with 1.25×10^5 (1×) and 5.0×10^5 (4×) cells and 3-D culture was continued for 2 weeks. Normal culture medium contained 1.0 mM Pi. *P < 0.05, ***P < 0.001: compared with the corresponding value for 1× cell density. Numbers of experiments are shown in parentheses.

Table 1

Sequences of the PCR primers used in the present study

	Forward (5′–3′)	Reverse (5′–3′)
ALP	TCCCAAAGGCTTCTTCTTGC	ATGGCCTCATCCATCTCCAC
Runx2	CAACCACAGAACCACAAGTGC	CACTGACTCGGTTGGTCTCG
OCN	TATGGCACCACCGTTTAGGG	CTGTGCCGTCCATACTTTCG
α-SMA	ACTGGGACGACATGGAAAAG	CATACATGGCAGGGACATTG
ACTB	GATCAAGATCATTGCTCCTCC	GTGTAAAACGCAGCCTCAGTA

GenBank accession numbers; ALP, NM_013059; Runx2, AF053950; OCN, NM_013414; α-SMA, NM_031004; ACTB, NM_031144.

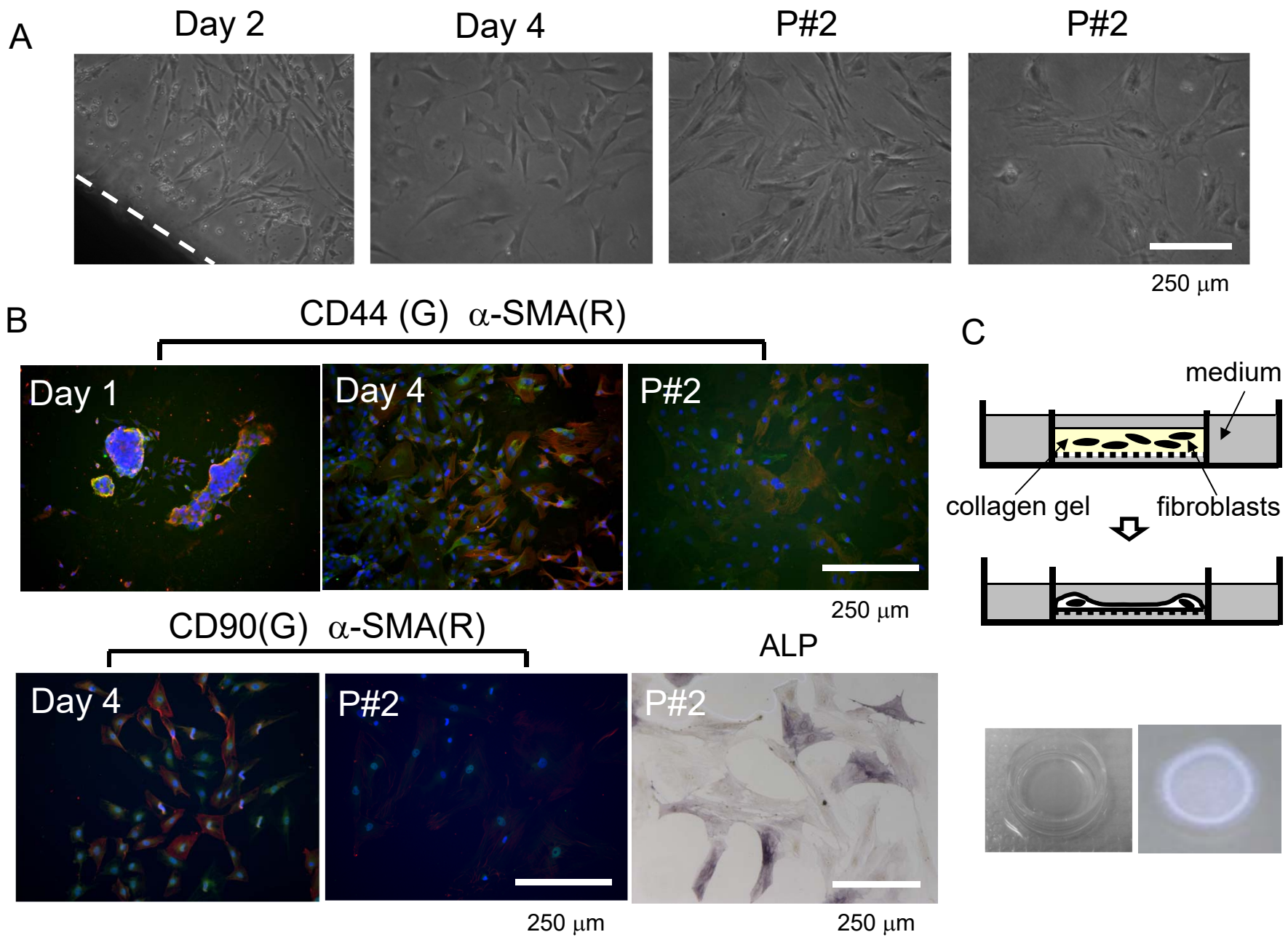

Fig. 1 Suyama *et al*.

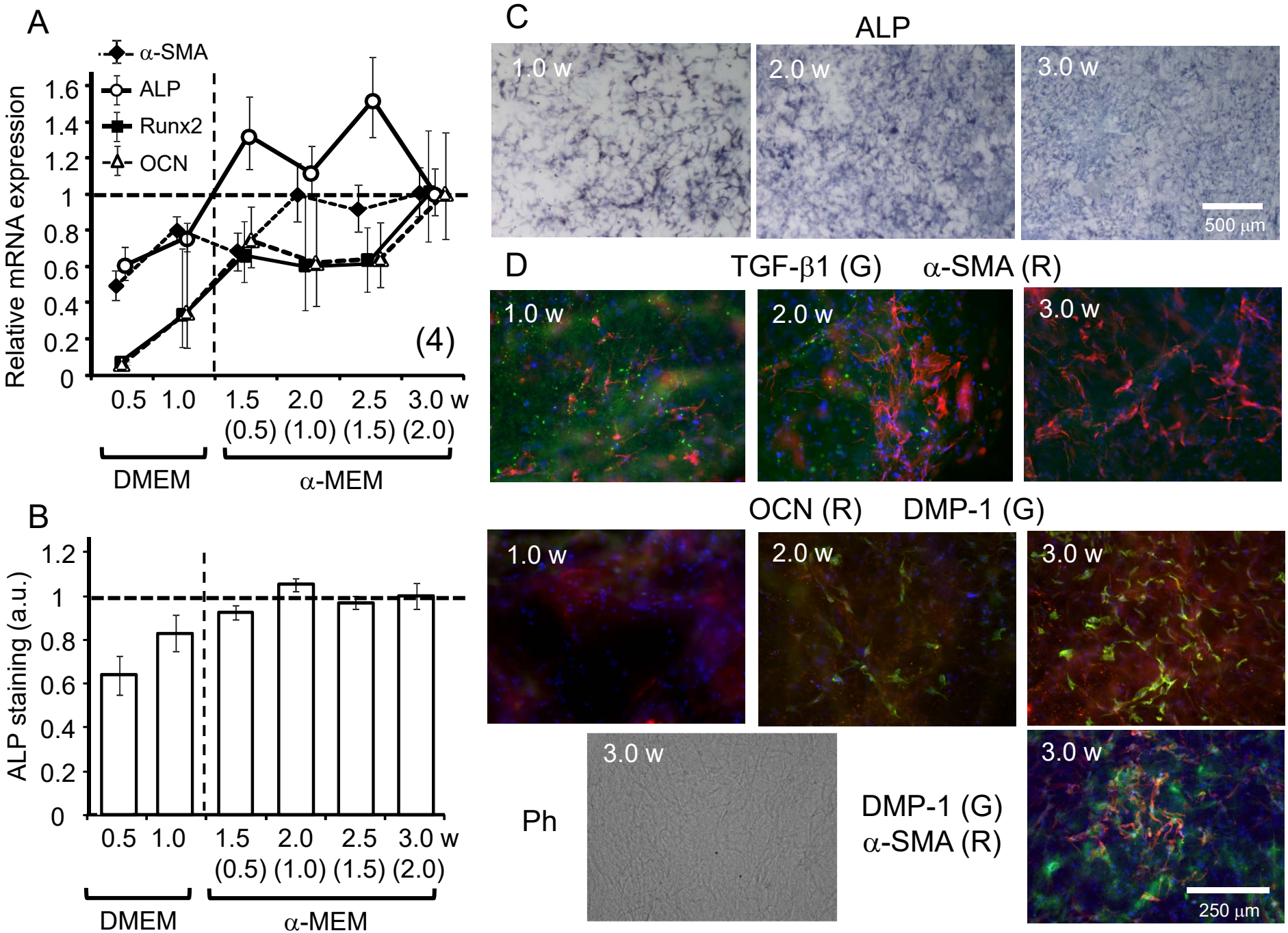

Fig. 2 Suyama *et al*.

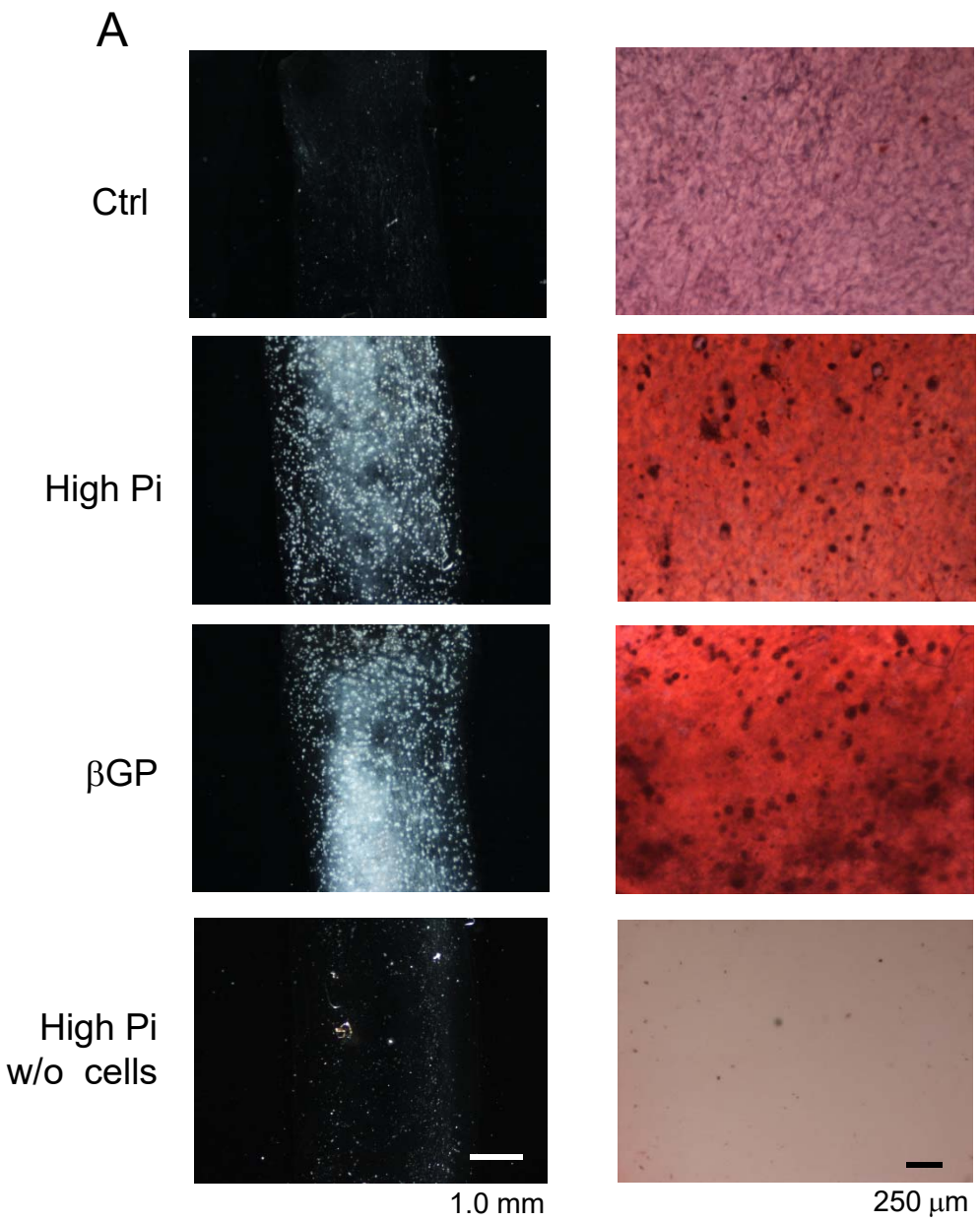

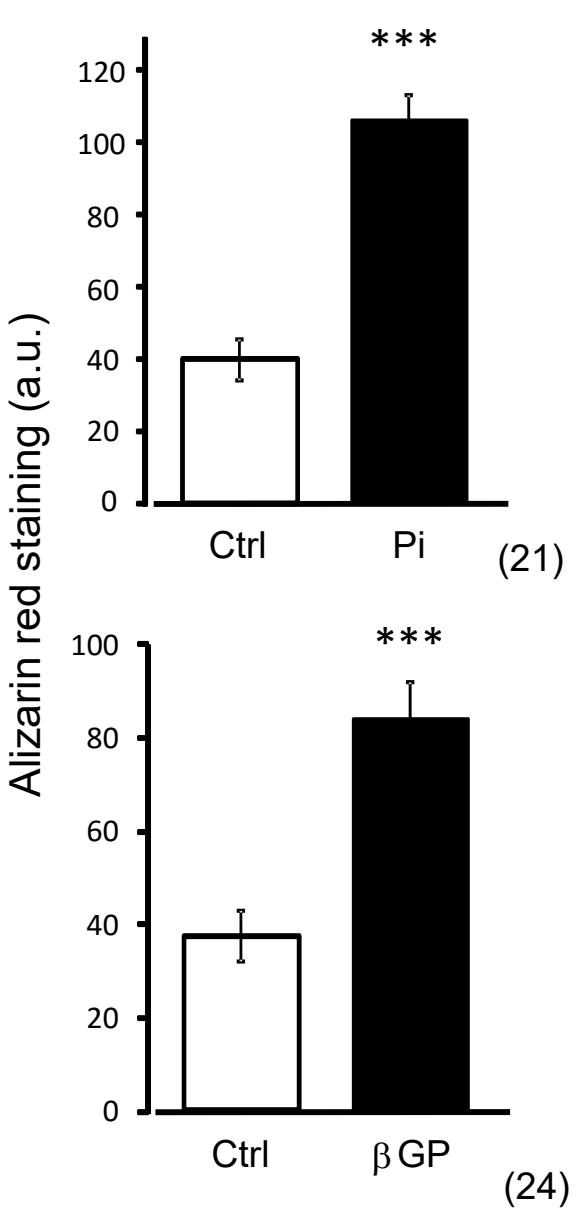

Fig. 3 Suyama *et al*.

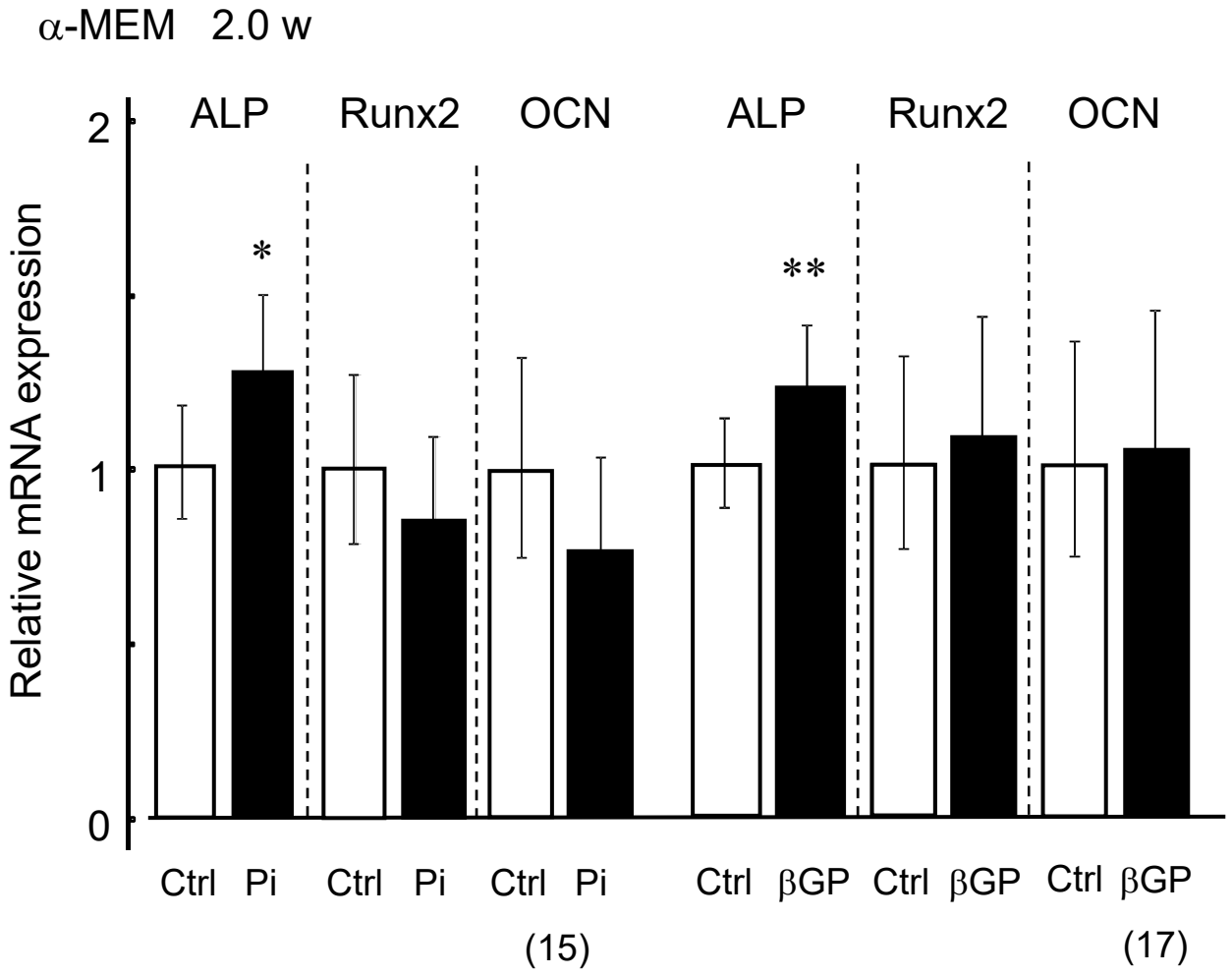

Fig. 4 Suyama *et al*.

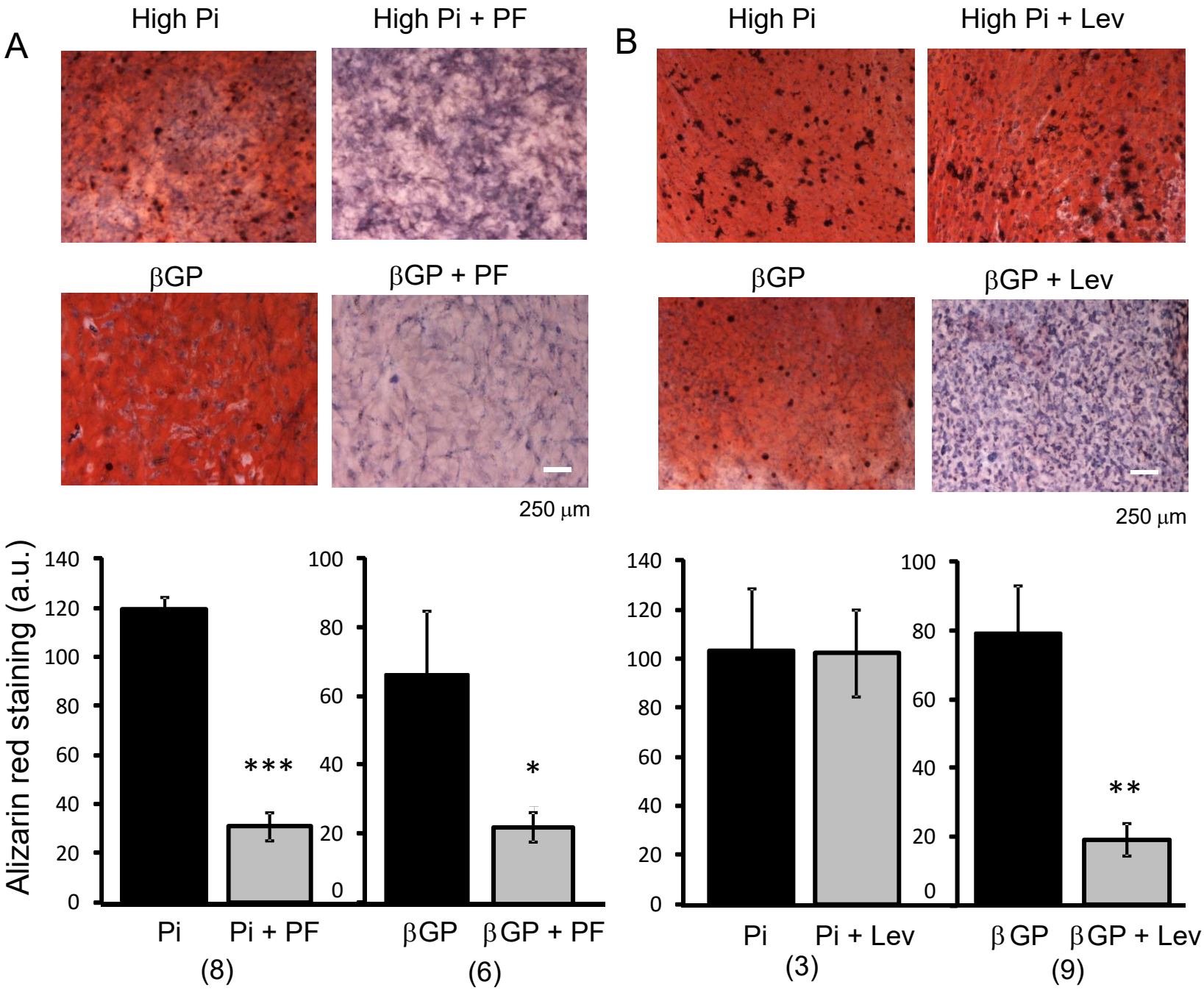

Fig. 5 Suyama *et al*.

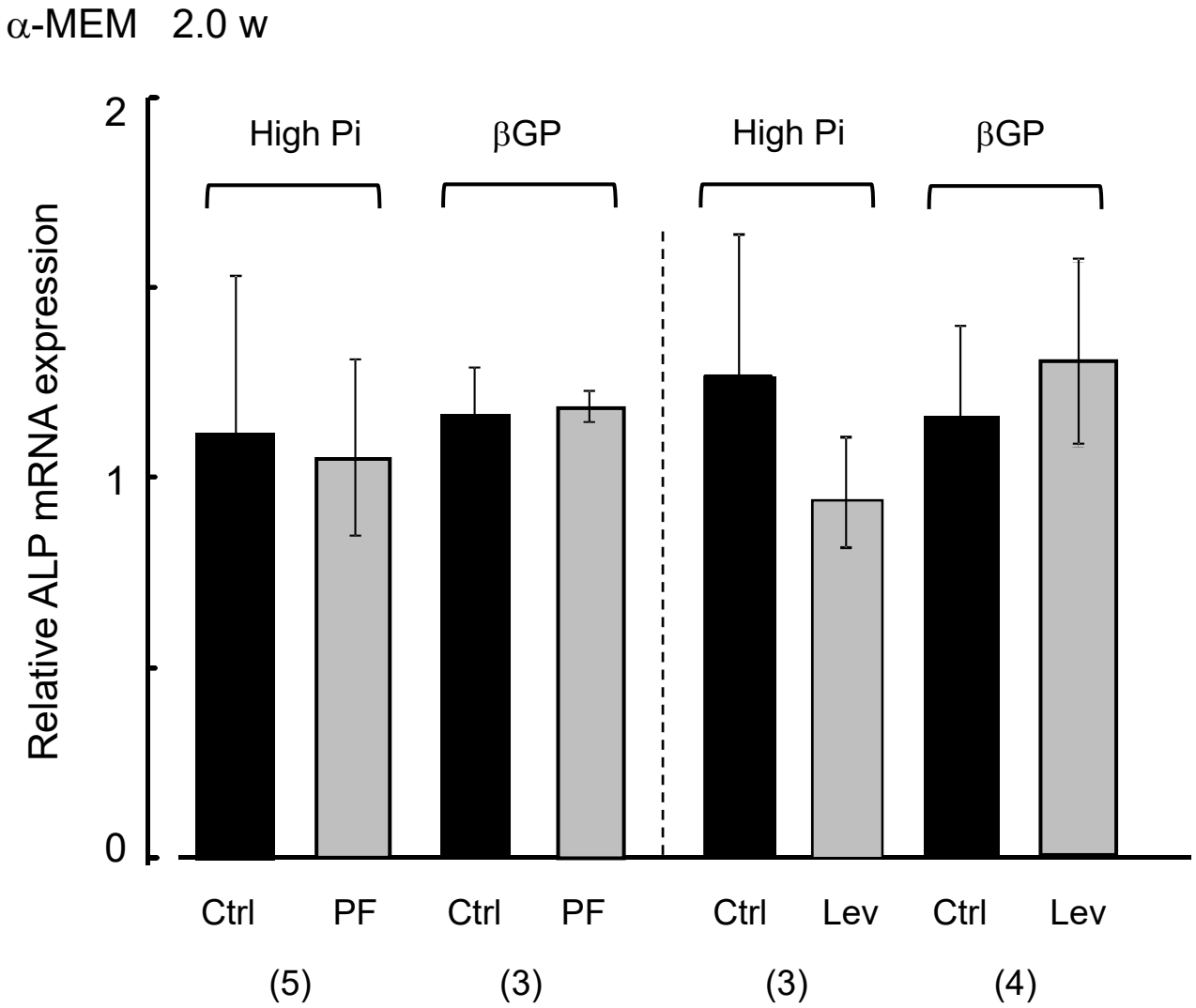

Fig. 6 Suyama *et al*.

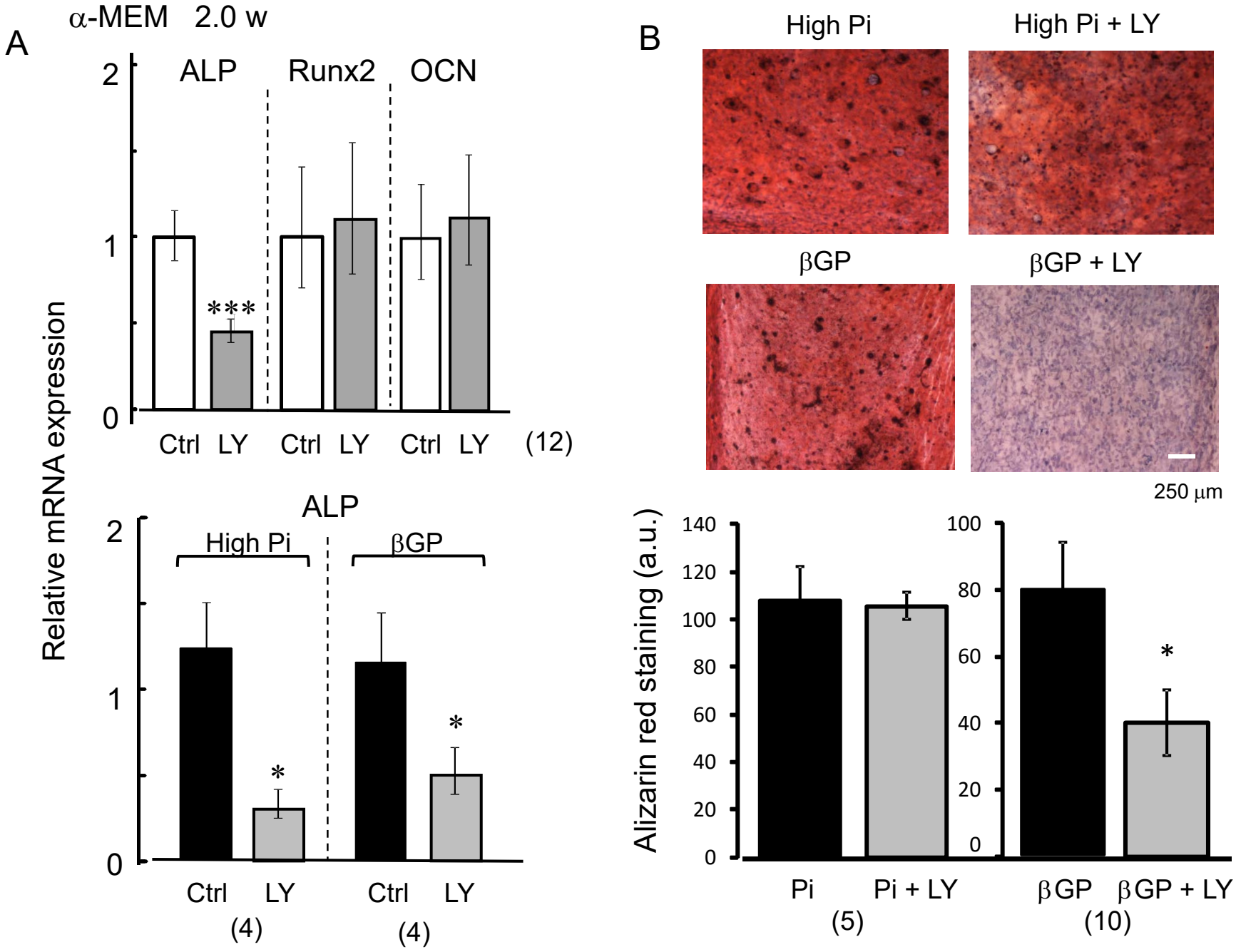

Fig. 7 Suyama *et al*.

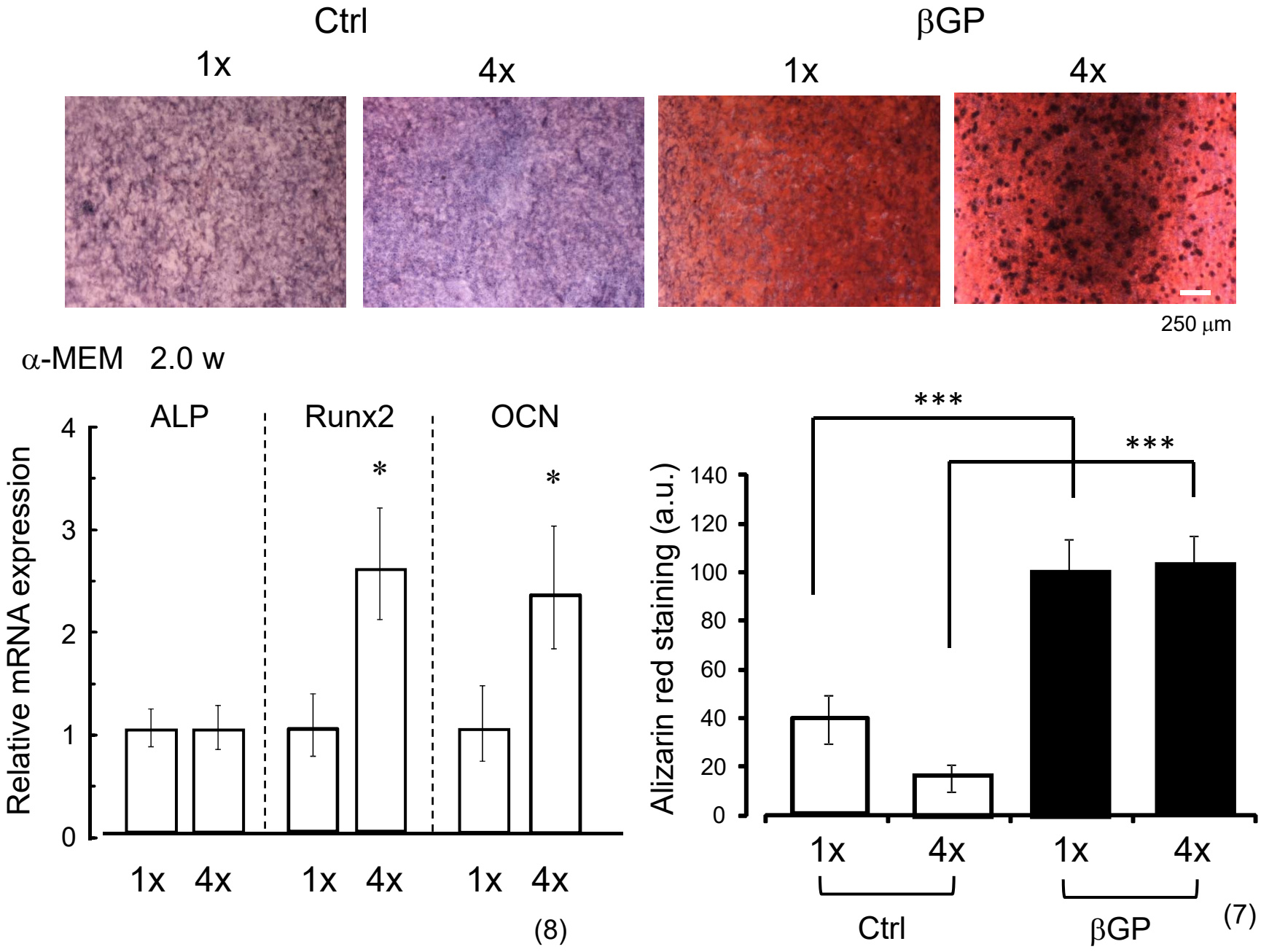

Fig. 8 Suyama *et al*.